

Jet Impingement onto a Dimpled Surface with Different Crossflow Schemes

Koonlaya KANOKJARUVIJIT¹ and Ricardo F. MARTINEZ-BOTAS²

¹ Postgraduate Student

Department of Mechanical Engineering
Imperial College London

Exhibition Road, South Kensington, London SW7 2BX ENGLAND

Phone: +44 (0)20 7594 7116, FAX: +44-(0)20 7823 8845, E-mail: koonlaya.kanokjaruvijit@imperial.ac.uk

²Department of Mechanical Engineering
Imperial College London

ABSTRACT

An eight-by-eight jet array impinging onto a staggered array of dimples, which was used as a turbulence promoter, at Reynolds number 11000 was investigated by the transient wide band liquid crystal method. The distance between the perforated plate and the target plate was adjusted to be 2, 4 and 8 jet diameters to examine its effect on the heat transfer performance. The effect of dimple geometry was considered with two different dimple configurations: hemispherical and cusped elliptical. Moreover, the effect of crossflow on jet deflection and heat transfer reduction was also investigated by either installing or removing sidewalls: one-way spent air exit, two-way spent air exit and four-way spent air exit. All heat transfer results were normalized by those from a flat surface at the same condition. Both normalized local and average heat transfer results are shown.

NOMENCLATURE

c	thermal capacity of Acrylic
D	jet diameter
h	heat transfer coefficient
H	distance measured from nozzle plate to flat portion of target plate
k	thermal conductivity of Acrylic
Nudimple	Nusselt number obtained from dimpled plate
Nuflat	Nusselt number obtained from flat plate
T _i	initial temperature of target plate right before impingement began
T _m	bulk fluid temperature
T _s	surface temperature
X	spanwise distance of target plate
Y	streamwise distance of target plate
ρ	density of Acrylic plate

INTRODUCTION

Jet impingement is a mature technique, which has been examined by many researchers as a method of heat transfer enhancement in a variety of applications. There have been a number of attempts to complement jet impingement with other enhancing techniques such as crossflow, ribs and turbulators. Attempts have been made to optimize each method in order to obtain effective heat transfer with low pressure loss. In order to augment the heat transfer, the boundary layer has to be thinned or be partially broken and restarted.

Regarding the flow passed dimples on their own, as a turbulence generator, a limited number of studies have been published. Kerarev and Kozlov (1993) studied the flow past a single hemispherical dimple of 150 mm diameter, and explained the flow pattern in terms of “sources” and “sinks”. The heat transfer was enhanced by 1.5 times compared to a plane circle of the same diameter. Afanasyev et al. (1993) investigated the effect of the density of a staggered-dimpled plate; they concluded that the density did not have an important effect on the flow hydrodynamic, but on the separation of temperature profile. The greater the density of the dimples on the streamline surface, the greater the deviation of the temperature profile was from the logarithmic law of wall. However, the heat transfer was increased by 30-40% without any significant increase in friction factor. They suggested that the viscous sublayer thickness was slightly decreased due to the concavities of the dimple. A heat transfer study of the flow past a staggered dimple passage was conducted by Moon et al. (1999) using the narrow-band transient liquid crystal method. They stated that the dimpled passage enhanced heat transfer by 2.1 times that of a smooth passage, while the friction factor was only 1.6-2 times more. There have been a number of studies on the effect of dimple geometry. Bearman and Harvey (1976) compared the lift and drag coefficients of hemispherical and hexagonal dimpled golf balls, and discovered that the hexagonal dimples caused more lift and slightly lower drag. This was because there were discrete vortices shed into the boundary layer. Chyu et al. (1997) investigated the effect of dimple geometry by comparing the heat transfer results of hemispherical and teardrop shaped dimples. The teardrop shaped dimples lead to higher heat transfer rates than the hemispherical dimples, but of course, induced a larger pressure loss due to their sharp angled part. The fluid mechanics of the flow past a staggered array of hemispherical dimples was examined by Mahmood et al. (2000) using smoke-wire technique to visualize the flow. Vortex shedding was observed, and it leads to an enhancement of heat transfer of 1.85 to 2.89 times relative to a flat plate.

Gau and Chung (1991) examined slot jet impingement on semi-cylindrical concave and convex surfaces varying the slot width to surface diameter ratios from 8 to 45 at Reynolds number from 6000 to 35000. Both cases enhanced heat transfer beyond impingement on a flat plate. Ekkad and Kontrovitz (2002) used a transient narrow band liquid

crystal technique to investigate jet impingement onto a hemispherical dimpled surface with dimple diameter-to-depth ratios of 0.125 and 0.25. Their dimple size was designed for the jet to impinge completely within the dimple. Their results showed that the appearance of dimples did not complement the jet impingement, but reduced the heat transfer, unlike the application of dimples to the passage flow.

The goal of the current research was to study the heat transfer performance of jet impingement onto a dimpled surface. A ratio of jet diameter-to-dimple diameter of 0.59 was used. The measurement technique was the transient wide band liquid crystal method. Dimples were used as turbulence promoters. The effect of dimple geometry on heat transfer was investigated using conventional hemispherical dimples as well as a new geometry in the form of a cusped elliptical shape. All results were compared with those of a flat surface in order to explain the consequence of the usage of dimples. Furthermore, the effect of crossflow scheme was studied to illustrate how each scheme affected the thermal transport.

EXPERIMENTAL APPARATUS AND PROCEDURES

A schematic of the experimental apparatus is shown in Fig. 1. The air was supplied by a fan, and heated up by a 9-kilowatt heater. A honeycomb sandwiched by two mesh screens inside the plenum chamber was used in order to straighten the flow. The experiment was transient, which required the airflow to settle before impinging, this was achieved with the help of a drawer that bypass the target plate. An eight-by-eight array of cylindrical holes was installed underneath the plenum chamber. The distance

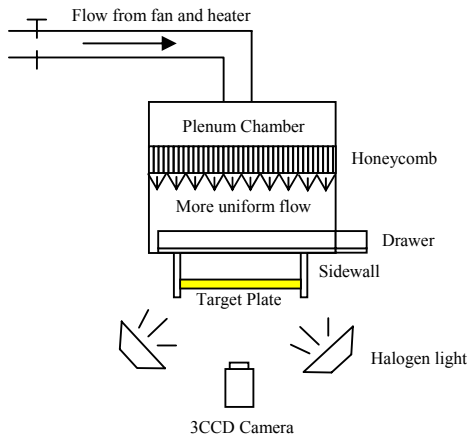


Fig. 1 Schematic of Experimental Apparatus

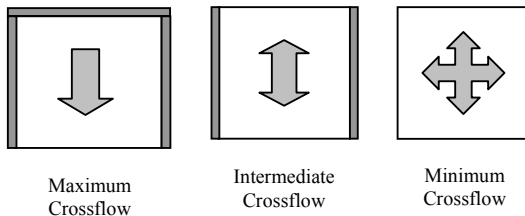
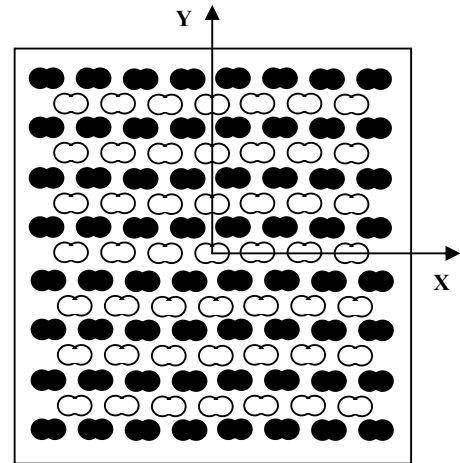
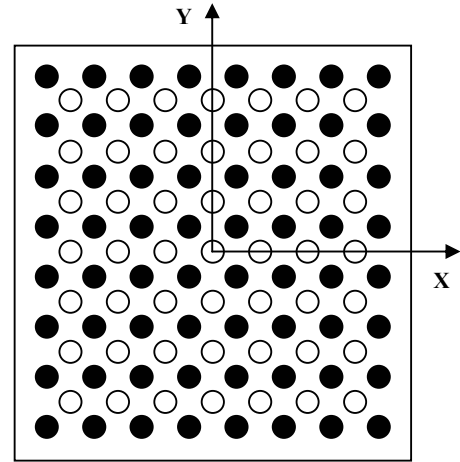
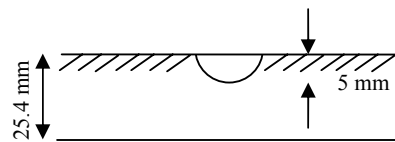


Fig. 2 Crossflow Schemes

between the perforated plate and the target plate (H/D) was adjusted to be 2, 4 and 8 jet-diameters. Sidewalls made of Acrylic plates were installed or removed when changing the crossflow schemes such as maximum, intermediate and minimum spent exits using studs as shown in Fig. 2.



● ● Impinging jet positions



Side view of dimpled plate

Fig.3 Hemispherical dimpled plate and cusped elliptical dimpled plate showing also the positions of impinging jets (Not to scale)

Two dimpled plates with the same wetted area for each dimple were tested: hemispherical and cusped elliptical shapes. Both were manufactured in staggered array on a square Acrylic plate of the size $320 \times 320 \times 25.4$ mm, illustrated in Fig. 3. The diameter of a hemispherical dimple was 17 mm, and each circle diameter of a cusp was 14.5 mm with the center-to-center distance of 8.74 mm. The inline array of nozzle holes were aligned with the eight-by-eight dimples as

shown in Fig. 3. The pitch of the dimples was 40 mm. Both plates were fabricated by using a ball mill and with the depth of 5 mm. A flat plate with the same dimension was also tested at the same conditions as a baseline. The cusped elliptical dimples were selected with the concept of the overlapping of two hemispherical dimples produced two sharp apices, which had potential of detaching the boundary layer better than round edges of regular hemispherical dimples as well as the consideration of simplicity in manufacturing.

Liquid crystals with a temperature range of 35 to 45°C, were applied on the Acrylic target plate. A SONY DCR-TRV 900E 3CCD camera was set up to take a picture from underneath with an off-axis fixed lighting installation. According to Camci *et al.* (1992) and Wang *et al.* (1994), hue is robust to the local light intensity and the illumination angle. It is also simple and monotonic function to the liquid crystal temperature, and, therefore, widely employed as a color index. In addition, it can easily be converted into accurate temperature distribution. MATLAB Image Processing Toolbox provided a convenient built-in function that converted RGB or Red-Green-Blue signal to HSV or Hue-Saturation-Value signal. The liquid crystal calibration of hue value against temperature was carried out for each target plate with the uncertainty within $\pm 3\%$. Nevertheless, the colors responding to the temperatures below 38°C conducted high uncertainty. The lower tail of the calibration curve was, then, retrenched in order to be able to use it with the real experiments. The curve fitting and regression analysis resulted in the fifth order polynomial temperature-hue relationship.

Each camera image was transferred to a personal computer using a firewire lead, which transferred data directly from the camera to the computer without the usage of a frame grabber. Each experiment was filmed with the non-compression mode in order to receive the data as complete as possible. Only the natural compression from the camera was allowed.

Since the transient method was applied throughout the research, the well known solution to the 1D unsteady heat conduction equation was used:

$$\theta = 1 - \exp(\beta^2 \operatorname{erfc} \beta) \quad (1)$$

$$\text{where } \theta = \frac{T_s - T_i}{T_m - T_i} \text{ and } \beta = \frac{h\sqrt{t}}{\sqrt{\rho c k}}$$

Only the flat areas outside dimples were considered for the image post-processing. The areas inside the dimples were not taken into account, these areas were, therefore, ineffective or out of interest.

The experimental uncertainty throughout this study was within $\pm 12.17\%$ based on 95% confidence levels according to Moffat (1990). The highest uncertainty that might happen was the sum of uncertainties of temperature measured by liquid crystals, the initial and the bulk flow temperatures measured by thermocouples, the time measured for taking a single frame (which was 1/25 second regarding the PAL system from the camera) and the thermal products from the Acrylic substrate, $\sqrt{\rho c k}$. As aforementioned, the temperature measured by liquid crystals has the uncertainty within $\pm 3\%$. Thermocouples used in this study had the uncertainty of $\pm 0.5^\circ\text{C}$, which made the uncertainties of initial and bulk flow temperatures become ± 2.5 and $\pm 1\%$, respectively. The highest uncertainty of time was $\pm 0.67\%$.

Finally, the uncertainty of the thermal properties of the Acrylic substrate was typically $\pm 5\%$.

RESULTS AND DISCUSSION

Overall average heat transfer of flat plate

The heat transfer results are presented as dimensionless Nusselt numbers at the specific Reynolds number of 11000. Fig. 4 shows the comparison of the results of a flat plate from this research to the literature; they agree well. As expected, the minimum crossflow scheme led to the highest heat transfer enhancement, followed by the intermediate crossflow scheme, and the maximum crossflow scheme gave the lowest results. It has been clearly explained by other researchers that strong crossflow causes heat transfer degradation, especially near the exit area, where the crossflow affected the most. The heat transfer results from the flat plate will be used as a baseline for those from dimpled surfaces hereafter.

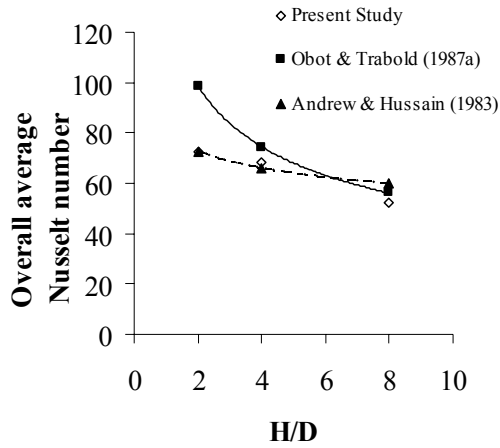
Fig.5 shows the spanwise and streamwise average Nusselt numbers of the flat plate for H/D of 8 for all schemes. The sidewalls, which confined the spent air to exit for the intermediate and maximum schemes, led to the heat transfer reduction. The symmetry of the heat transfer patterns in both spanwise and streamwise directions occurred in the minimum and intermediate schemes as the sidewalls conducted the spent air to. However, in the maximum crossflow scheme, the stagnation peaks were shifted and reduced in the streamwise direction by the strong crossflow degradation.

Effect of crossflow scheme on dimpled surfaces

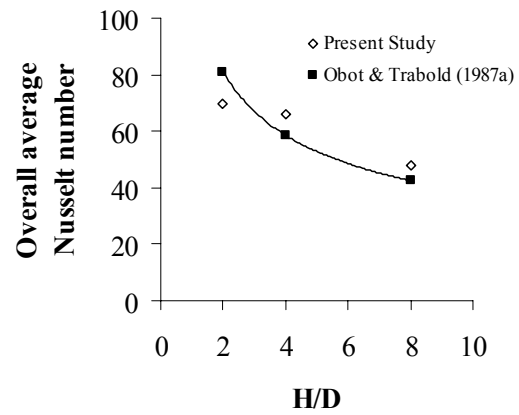
Throughout in this study, the jets impinged on dimples with the idea of employing the edges of dimples to thin the boundary layer, and enhance the heat transfer of the flat portions between dimples. The lowest heat transfer was expected inside each dimple similar to the parallel flow past dimples investigated by Mahmood *et al.* (2000) and to the study of Kesarev and Kozlov (1993) on a single dimple.

At H/D of 2 in both dimple geometries, both the intermediate and maximum crossflow schemes conducted heat transfer slightly less than the minimum crossflow scheme as shown in Figs.6 and 7. The coupled effects of impingement and channel flow could explain this. According to Cornaro *et al.* (1999), jet impinging on a concave surface led to the vortical fluid either axially or radially upward or both. For the minimum crossflow scheme, impingement dominated, since there was no sidewall to constrain the flow, but it freely exits. However, a recirculation region occurs inside the dimples, and small vortices are generated before subsequent breakdown (Cornaro *et al.*, 1999). After the jets impinged on the dimples, the crossflow was not strong enough to entrain the recirculating flow, while the spent air could not exit fast enough.

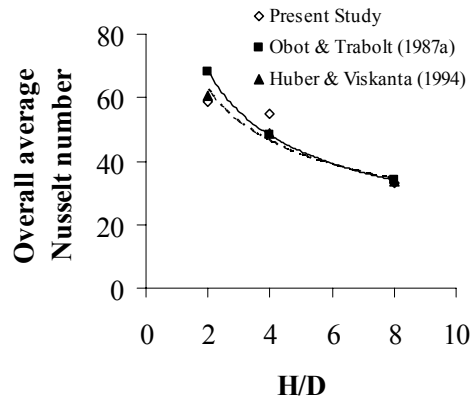
Figure 8 shows the contour distribution of the Nusselt number on hemispherical dimples for the maximum crossflow with H/D of 8. Note that the flow direction is from the bottom upwards. As aforementioned, the areas inside dimples were not taken into account. In this case, the crossflow deflected the oncoming jets, and impacted on downstream halves of dimples. The channel flow was formed and overwhelmed the impingement. As a consequence the boundary layer was thinned downstream of dimples leading to heat transfer enhancement. The flat areas adjacent to the dimples show the highest heat transfer enhancement.



(a) Maximum crossflow scheme



(b) Intermediate crossflow scheme



(c) Minimum crossflow scheme

Fig.4 Comparison to literature

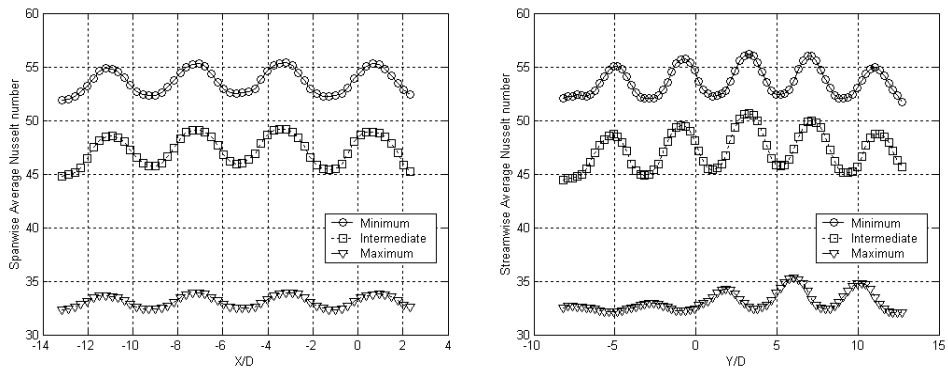


Fig. 5 Spanwise (left) and streamwise (right) average Nusselt numbers for flat plate at H/D of 8

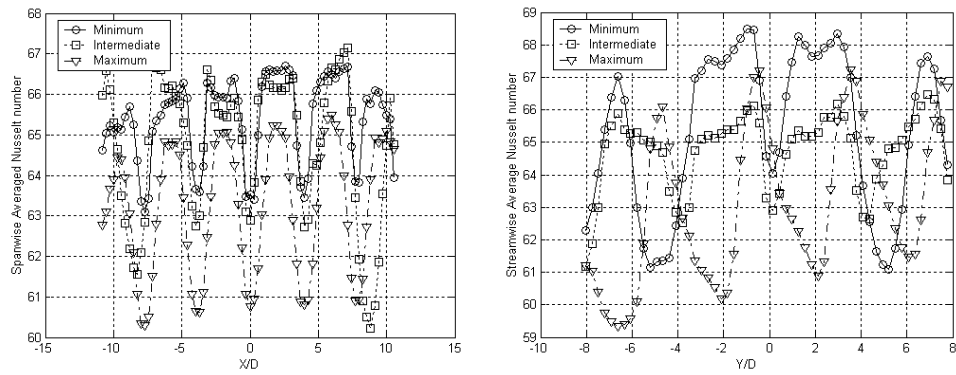


Fig. 6 Spanwise (left) and streamwise (right) average Nusselt numbers for hemispherical dimpled plate at H/D of 2

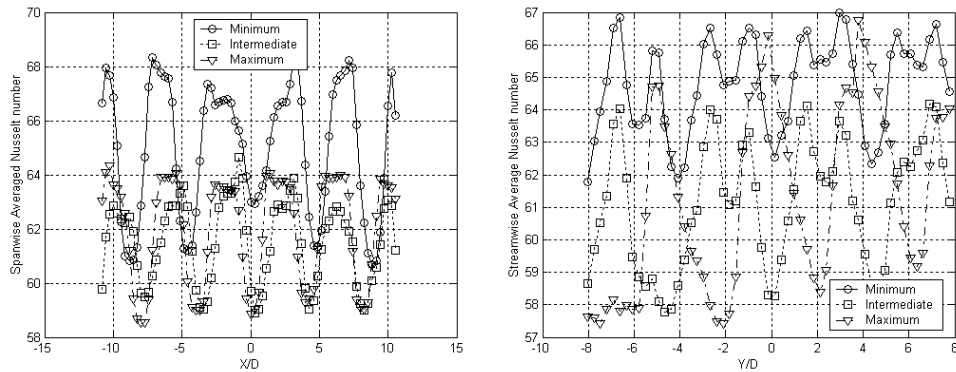


Fig. 7 Spanwise (left) and streamwise (right) average Nusselt numbers for cusped elliptical dimpled plate at H/D of 2

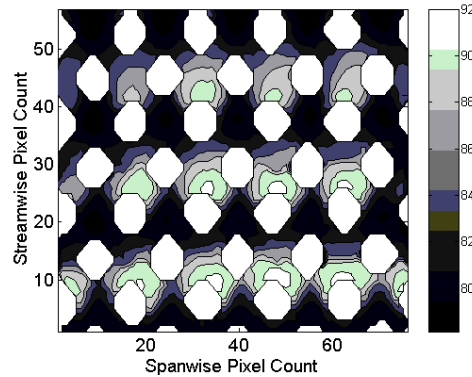
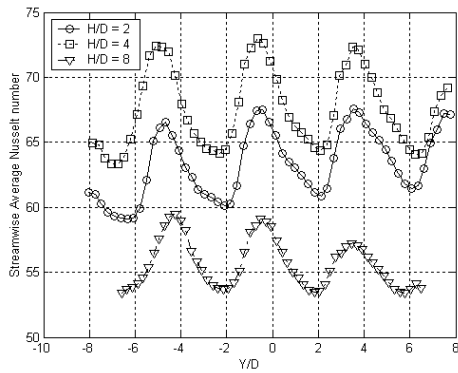


Fig. 8 Local Nusselt number distribution, hemispherical dimpled plate, maximum crossflow, H/D = 8

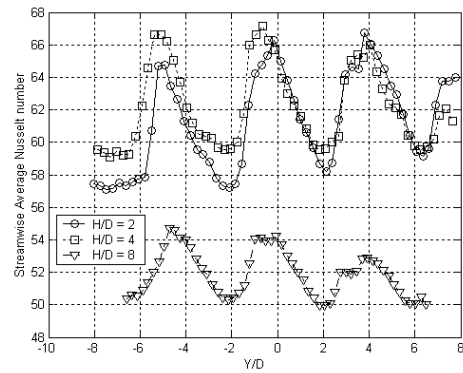
Effect of jet-to-plate spacing

The jet-to-plate spacing strongly affected the heat transfer results. For all crossflow schemes on the flat plate, the narrower the jet-to-plate spacing, the higher the heat transfer, which prior researchers have showed. For the dimpled plates, the heat transfer information did not follow the tendency of the flat plate, especially, for the minimum crossflow scheme in both dimpled plates. The highest Nusselt numbers occurred in the jet-to-plate spacing of 4 as shown in Fig. 9. The distance from the nozzle plate to the bottom of a dimple was 45 mm, which might be the end of the potential core. According to the flow visualization shown by Cornaro et al. (1999), at the end of the potential core, the strong radial

oscillation of the stagnation point accelerated the breakdown of the vortices that struck the surface, and this ruined the symmetry of the jet making it dissimilar to impingement on a flat plate. However, at the closer spacing, such as H/D of 2, even though the higher impact than other jet-to-plate spacing was expected, the strong recirculation might occur inside the dimples, and without the powerful channel flow formed for the freely exit scheme, the recirculating flow could not escape fast enough from each dimple. Therefore, the heat transfer measured from the flat portions of this case presented lower than H/D of 4, which is clearly seen for the hemispherical dimples.



(a) Hemispherical Dimples



(b) Cusped Elliptical Dimples

Fig. 9 Streamwise average Nusselt numbers for maximum crossflow scheme

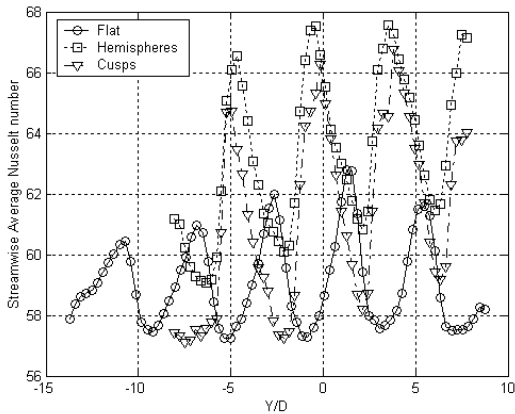
Effect of dimple geometry

Both dimple geometries were designed based on the same wetted cross sectional area or equivalent diameter with the same depth. Fig.10 shows the comparison of the streamwise average Nusselt numbers for the maximum crossflow scheme at all jet-to-plate spacing of all geometries.

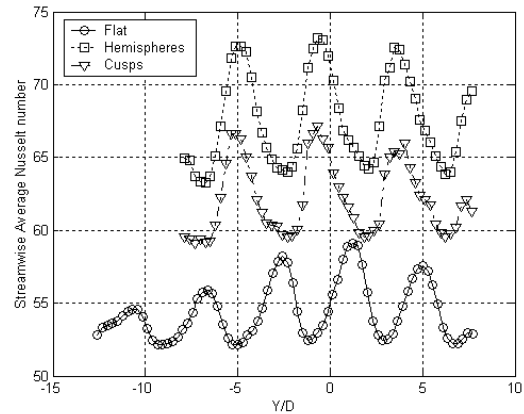
For H/D of 2, the hemispherical dimples performed slightly better than the cusped elliptical dimples by 2.79 % on average, 10.78 % for H/D of 4 and 6.70% for H/D of 8. This might be because when the jets impinged on the hemispherical dimples, the recirculation inside both dimples that formed a cusped elliptical dimple was less severe than that inside each cusped elliptical dimple. In addition, the potential core was possibly slightly longer than four jet diameters as mentioned in the previous section. Each jet impinging on an intersection between two dimples that formed a cusped ellipse, and this could split the flow into two parts,

which later produced a recirculating flow in each dimple. The two rolling-up recirculations disturbed the oncoming jet. However, since the three sidewalls constrained the spent air to form a channel flow, this might hasten the recirculation flow to shed along the crossflow. Hence, the degradation was not as severe in this shape compared to the other crossflow schemes. H/D of 8 for both geometries performed better than the other two spacings. The circulation inside each dimple, of course, was less strong and the edges of dimples might help thinning the boundary layer more effectively. Further flow visualization is needed to complete this physical explanation.

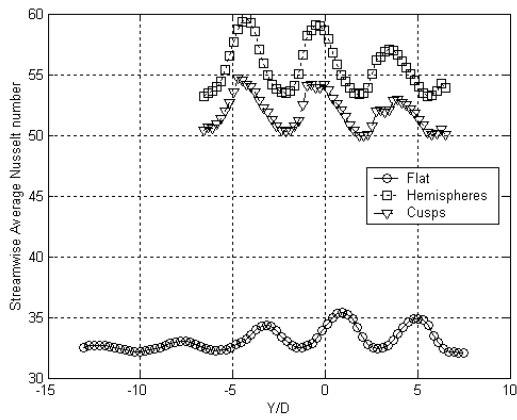
Nevertheless, in terms of economy, manufacturing and performance, the hemispherical shape is more attractive than the cusped elliptical shape. There are more parameters to determine the optimum such as dimple depth, ratio of jet diameter to dimple diameter (curvature) and position of impinging jets on the dimpled plate.



(a) H/D = 2



(b) H/D = 4



(c) $H/D = 8$

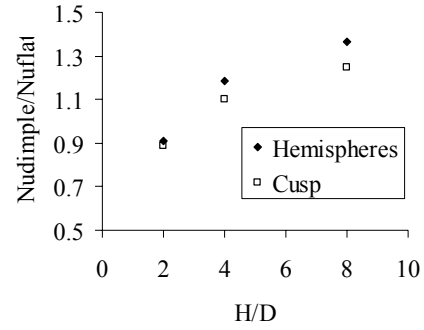
Fig. 10 Plots of streamwise normalized average Nusselt numbers of both dimpled plates for maximum crossflow scheme

Overall average Nusselt numbers of Dimples Plates

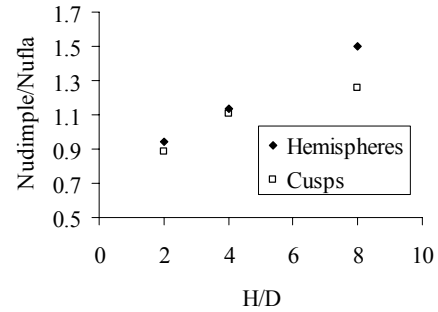
Throughout the study, the jets impinging on dimples, and the areas inside were not taken into account as mentioned in the previous section. However, the video exhibited that the lowest heat transfer occurred inside each dimple. In the minimum and intermediate crossflow schemes for H/D of 2, the presence of dimples did not help, but reduced the heat transfer by 10%. With the jet-to-plate spacing of 4 for minimum crossflow, the overall average heat transfer of the impingement on dimples was not different from that of the flat plate. By overall average, the heat transfer was more enhanced with the maximum crossflow and larger jet-to-plate spacing. From the prior researches in augmenting heat transfer of parallel flow using dimples, it could be inferred on the dimple impingement that the crossflow that formed a channel flow would have made a greater contribution of heat transfer enhancement. For the intermediate crossflow scheme, the dimpled plates enhanced heat transfer by 10 % for H/D of 4, and 30 to 50 % for H/D of 8 compared to that of the flat plate. The heat transfer was increased with the dimple application for the maximum crossflow schemes from 56 to 68 %. The flow mechanism of dimple impingement might be considered as a coupled effect of jet impingement and channel flow with vortex shedding occurred in the staggered dimple array as mentioned in the prior sections. At the higher jet-to-plate spacings (4 and 8), compared to a flat plate, the heat transfer was more enhanced with the presence of dimples. The potential core occurred possibly at the end of H/D of 4, in addition, the depth of each dimple ensured the end of the potential core was reached. The dimples aided the impingement by thinning or disturbing the boundary layer. However, the recirculation inside dimples was also concerned for degrading the heat transfer, especially the results shown in H/D of 2.

CONCLUSIONS

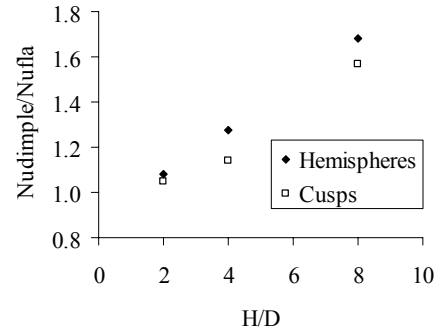
Impingement onto dimples performed best with the maximum crossflow scheme and larger jet-to-plate spacing due to the coupled effect of impingement and channel flow. The heat transfer on the downstream half of a dimple edge was higher than the upstream half. This occurred in maximum crossflow scheme, however, in minimum and crossflow schemes, the impingement overwhelmed the channel flow. For the intermediate crossflow scheme, either



(a) Minimum Crossflow



(b) Intermediate Crossflow



(c) Maximum Crossflow

Fig. 11 Overall average normalized Nusselt numbers

phenomenon could not perform at its high capacity, but seems to act moderately.

Since the jet impingement on dimples caused the recirculation inside the dimples, and this affected enormously on the case of narrow jet-to-plate spacing ($H/D = 2$), the heat transfer was aggravated comparing to that of the flat plate. However, the channel flow formed by the intermediate and maximum crossflow schemes helped diminishing this deterioration especially on H/D of 4 and 8.

Finally, the investigation on the effect of dimple geometry showed that hemispherical and a cusped elliptical dimple did not perform immensely differently. However, comparing in terms of economy, manufacturing and pressure loss, the hemispherical shape should be a better choice. Nevertheless, since the application of dimpled surface to jet

impingement has just begun recently, the optimum of some parameters should be researched such as dimple depth, ratio of jet diameter to dimple diameter (curvature) and position of impinging jets on the dimpled plate as well as the qualitative flow visualization.

REFERENCES

- Afanasyev, V.N., Chudnovsky, Ya.P., Leontiev, A.I., and Roganov, P.S., 1993, "Turbulent Flow Friction and Heat Transfer Characteristics for Spherical Cavities on a Flat Plate", *Experimental Thermal and Fluid Science*, Vol.7, pp.1-8.
- Andrews, G.E., Hussain, C.I., 1983, "Impingement Cooling of Gas Turbine Component", Tokyo International Gas Turbine Congress and Exhibition.
- Babinsky, H., and Edwards, J.A., 1996, "Automatic Liquid Crystal Thermography for Transient Heat Transfer Measurements in Hypersonic Flow", *Experiments in Fluids*, Vol.21, pp.227-236.
- Bearman, P.W., and Harvey, J.K., 1976, "Golf Ball Aerodynamics", *Aeronautical Quarterly*, May 1976, pp.112-122.
- Camci, C., Kim, K., and Hippensteele, S.A., 1992, "A New Hue Capturing Technique for the Quantitative Interpretation of Liquid Crystal Images Used in Convective Heat Transfer Studies", *Journal of Turbomachinery*, Vol. 114, pp. 765-775.
- Cornaro, C., Fleischer, A.S., Goldstein, R.J., 1999, "Flow visualization of a round jet impinging on cylindrical surfaces," *Experimental Thermal and Fluid Science*, 20, pp.66-78.
- Chyu, M.K., Yu, Y., Ding, H., Downs, J.P., and Soechting, F.O., 1997, "Concavity Enhanced Heat Transfer in an Internal Cooling Passage," ASME Paper, 97-GT-437.
- Gardon, R., and Akfirat, J. C., 1965, "The role of turbulence in determining the heat-transfer characteristics of impinging jets", *International Journal of Heat Mass Transfer*, Vol. 8, pp.1261-1272.
- Gau, C., and Chung, C.M., 1991, "Surface curvature effect on slot-air-jet impingement cooling flow and heat transfer process," *Journal of Heat Transfer*, 113, pp.858-864.
- Goldstein, R.J., and Timmers, J.F., 1982, "Visualization of Heat Transfer from Arrays of Impinging Jets," *International Journal of Heat Mass Transfer*, Vol. 25, No. 12, pp.1857-1868.
- Huber, A.M., and Viskanta, R., 1994a, "Convective Heat Transfer to a Confined Impinging Array of Air Jets with Spent Air Exits," *Journal of Heat Transfer*, Vol. 116, pp.570-576.
- Huber, A.M., and Viskanta, R., 1994b, "Effect of Jet-Jet Spacing on Convective Heat Transfer to Confined, Impinging Arrays of Axisymmetric Air Jets", *International Journal of Heat Mass Transfer*, Vol.37, No.18, pp.2859-2869.
- Kesarev, V.S., and Kozlov, A.P., 1993, "Convection Heat Transfer in Turbulized Flow Past a Hemispherical Cavity", *Heat Transfer Research*, Vol. 25, No. 2, pp.156-160.
- Kline, S.J., and McClintock, F. A., 1953, "Describing uncertainties in single-sample experiments", *Mechanical Engineering*, January, pp.3-8.
- Lee, K. C. and Yianneskis, M., 1993 "An Image processing technique for the analysis of thermotic distributions utilising liquid crystals", *Imaging in Transport Processes*, chapter 3, pp. 195-202.
- Mahmood, G. I., Hill, M. L., Nelson, D. L., and Ligrani, P. M., 2000 "Local Heat Transfer and Flow Structure on and above a Dimpled Surface in a Channel", *ASME International Gas Turbine and Aeroengine Congress and Exhibition*, Germany, May 8-11, 2000, 2000-GT-230.
- Moffat, R., 1990, "Experimental Heat Transfer", 9th International Heat Transfer Conference, Jerusalem, Israel.
- Moon, H.K., O'Connell, T., and Glezer, B., 1999, "Channel Height Effect on Heat Transfer and Friction in a Dimpled Passage", ASME Paper, 99-GT-163.
- Obot, N.T., and Trabold, T.A., 1987a, "Impingement Heat Transfer within Arrays of Circular Jets: Part I- Effects of Minimum, Intermediate and Complete Crossflow for Small and Large Spacings", *Journal of Heat Transfer*, Vol. 109, pp.872-879.
- Obot, N.T., and Trabold, T.A., 1987b, "Impingement Heat Transfer within Arrays of Circular Jets: Part II- Effects of Crossflow in the Presence of Roughness Elements", ASME Paper, 87-GT-200.
- Van Treuren, K.W., Wang, Z., Ireland, P.T., and Jones, T.V., 1994, "Detailed Measurements of Local Heat Transfer Coefficient and Adiabatic Wall Temperature Beneath an Array of Impinging Jets," *Journal of Turbomachinery*, Vol. 116, pp. 369-374.
- Wang, Z., Ireland, P.T., Jones, T.V., and Davenport, R., 1994, "A Colour Image Processing System for Transient Liquid Crystal Heat Transfer Experiments", ASME Paper, 94-GT-290.
- Wang, Z., Ireland, P.T., Kohler, S.T., and Chew, J.W., 1998, "Heat Transfer Measurements to a Gas Turbine Cooling Passage with Inclined Ribs," *Journal of Turbomachinery*, Vol.120, pp.63-69.